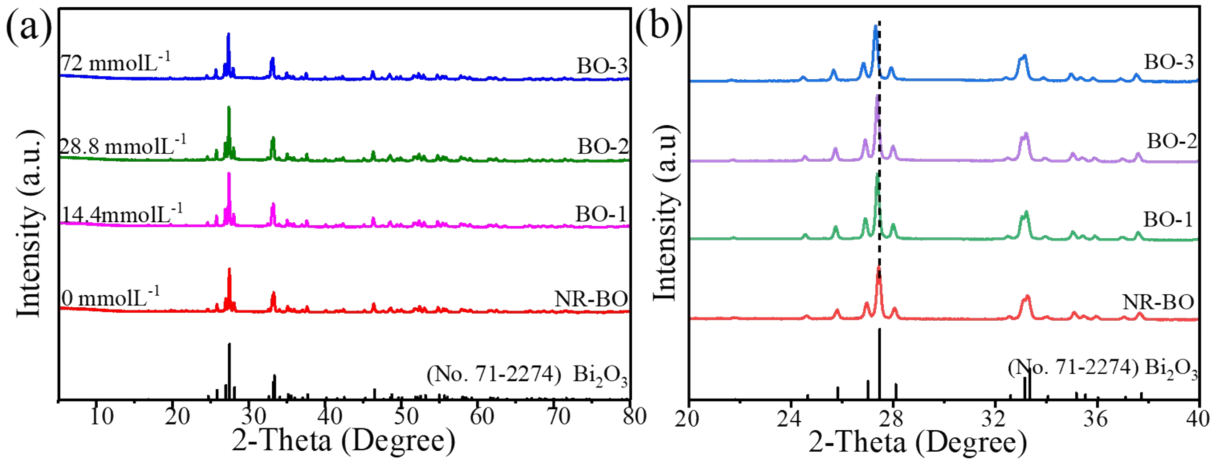

Fig. S1 XRD patterns of the obtained samples with different concentrations of nitric acid.

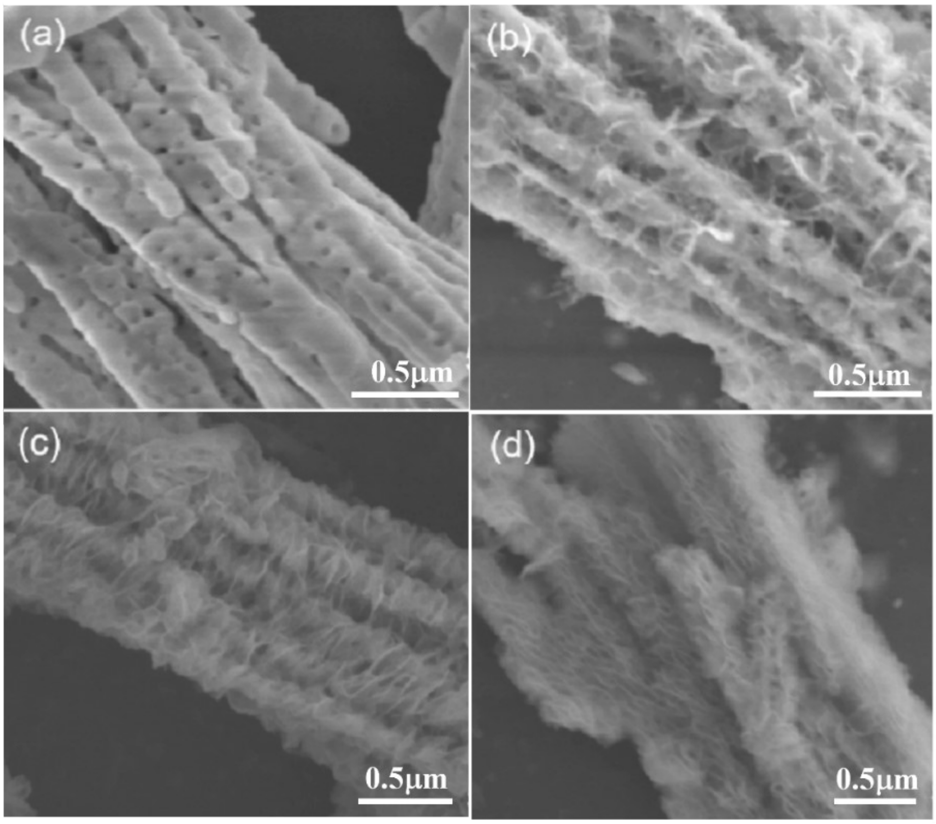

Fig. S2 SEM images of the obtained samples with different concentration of nitric acid, (a) 0 mmol•L^{-1}, (b) 14.4 mmol•L^{-1}, (c) 28.8 mmol•L^{-1}, (d) 72 mmol•L^{-1}.

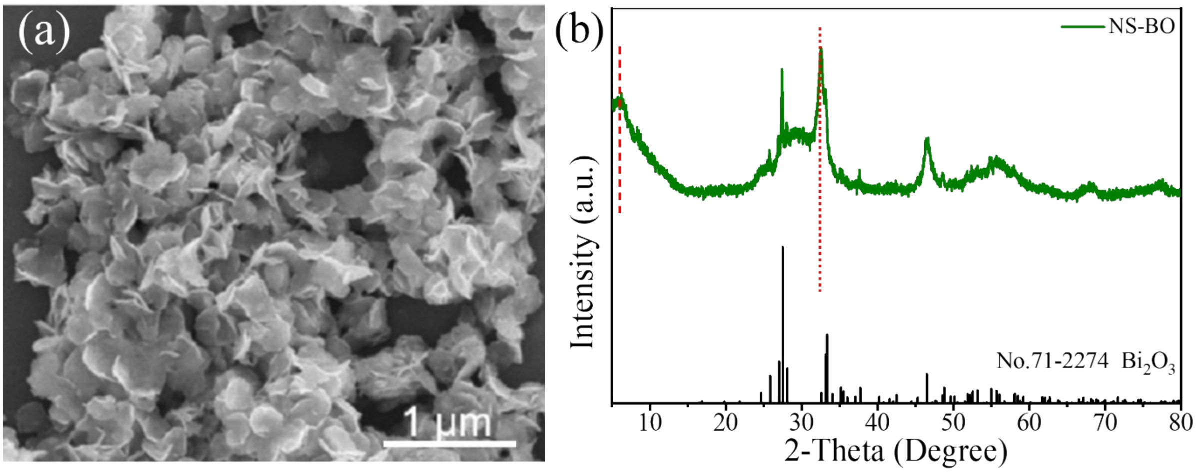

Fig. S3 SEM photographs (a) and XRD pattern (b) of BO-NS, C_{HNO_3} = 288 mmol•L^{-1}.

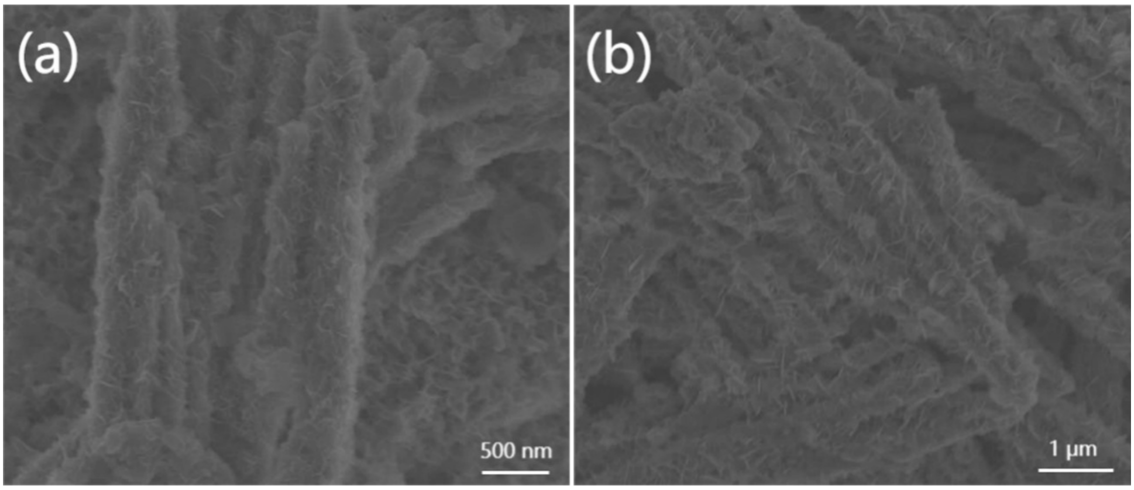

Fig. S4 SEM images of BO-2 synthesized at (a) 40 °C and (b) 60 °C, respectively.

Table S1 Comparison of the photoreduction Cr (VI) (Xe lamp, 300 W).

Materials	Catalyst dosage (g/L)	$C_{Cr(VI)}$ (mg/L)	Illumination time/ Reduction efficiency	k/ min^{-1}	ref
Cl-doped Bi_2S_3 homojunction	0.2	10	70 min/96.6%	0.036	[1]
0D/1D Bi_2MoO_6	0.6	20	80 min/100%	0.024	[2]
α/γ In_2Se_3	0.2	100	10 min/94.9%	0.239	[3]
p-n style TiO_2	0.75	15	60 min/91%		[4]
In_2S_3 Homojunction	0.4	20	30 min/98%	0.13	[5]
$Bi_4V_2O_{11}$ Homojunction	0.5	10	100 min/87%		[6]
QDs self-decorated Bi_2MoO_6	0.5	10	20 min/60%	0.047	[7]
Anatase-rutile TiO_2	0.5	10	40 min/82%	0.046	[8]
$Zn_3In_2S_6$/ Bi_2O_3	0.5	10	120 min/99.8%	0.054	[9]
Bi_2O_3/$CuBi_2O_4$/Ag	0.4	10	30 min/96.9%	0.115	[10]
Bi_2O_3QDs/g-C_3N_4	0.5	10	60 min/87.9%	0.033	[11]
Bi_2O_3/g-C_3N_4	0.5	10	180 min/90%	0.01	[12]
Bi_2O_3/BiOI	0.2	20	100 min/94.5%		[13]
SnO_2/ Bi_2O_3/BiOI	0.5	50	120 min/90%		[14]
P-doped BiO_x	0.5	5	180 min/84%		[15]
AgI/BiOI- Bi_2O_3	1.0	10	90 min/98%	0.032	[16]
Bi_2O_3 porous nanosphere	1.0	40	20 min/100%		[17]
Bi_2O_3/red P	0.25	40	30 min/99%	0.118	[18]
Bi_2O_3/Co_3O_4 @C	0.8	20	120 min/100%		[19]
β- Bi_2O_3/BiOCl	1.0	50	18 min/100%		[20]
β- Bi_2O_3@Bi_2S_3	0.5	20	60 min/100%		[21]
Bi_2O_3	1.0	50	10 min/100%	0.331	[22]
α-Bi_2O_3/α-Bi_2O_3	1.0	50	6 min/100%	0.657	This work
	1.0	100	12 min/100%	0.207	
	0.5	50	15 min/100%	0.166	

Table S2 Apparent rate contents (k) and BET surface area.

Samples	BET surface area (m^2•g^{-1})	k(min^{-1})	k'(k/BET)
		Cr(VI)	Cr(VI)
BO-NR	7.9617	0.069	0.0087
BO-2	25.4538	0.657	0.0258
BO-3	43.8680	0.490	0.0112

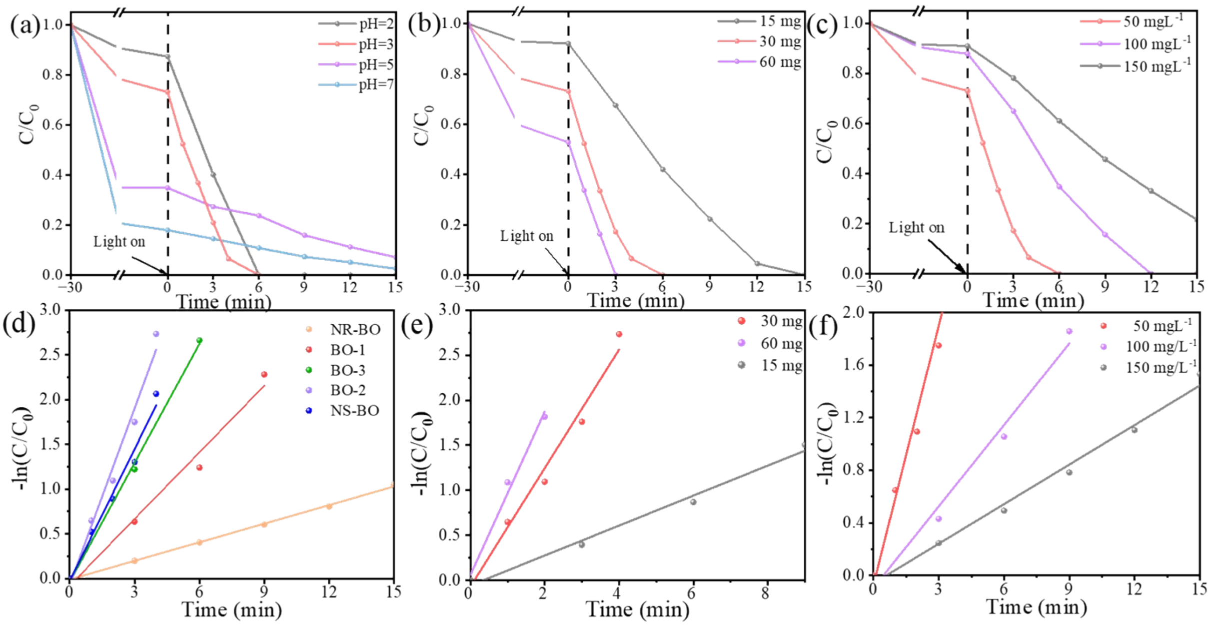

Fig. S5 (a) The reduction curve of Cr(VI) (50 mg•L^{-1}) at different pH values, (b) the effect of different dosage of BO-2 on reduction of Cr(VI) (50 mg•L^{-1}), (c) different concentrations Cr (VI) solutions with BO-2; The first-order kinetic curve for degrading Cr(VI). (d) Cr(VI) (50 mg•L^{-1}), (e) different amount of BO-2 photocatalyst, (f) different concentration of Cr(VI) using BO-2 (30 mg) as photocatalyst.

Table S3 Reaction rate contents (k) under different conditions.

	Cr(VI) (50 mg•L^{-1})			
	NR-BO	BO-1	BO-3	BO-2
k/min^{-1}	0.06925	0.248	0.443	0.657

	Cr(VI) (50 mg•L^{-1})		
	15 mg (BO-2)	30 mg (BO-2)	60 mg (BO-2)
k/min^{-1}	0.166	0.657	0.907

	30 mg BO-2 photocatalyst		
	50 mg•L^{-1} Cr(VI)	100 mg•L^{-1} Cr(VI)	150 mg•L^{-1} Cr(VI)
k/min^{-1}	0.657	0.207	0.100

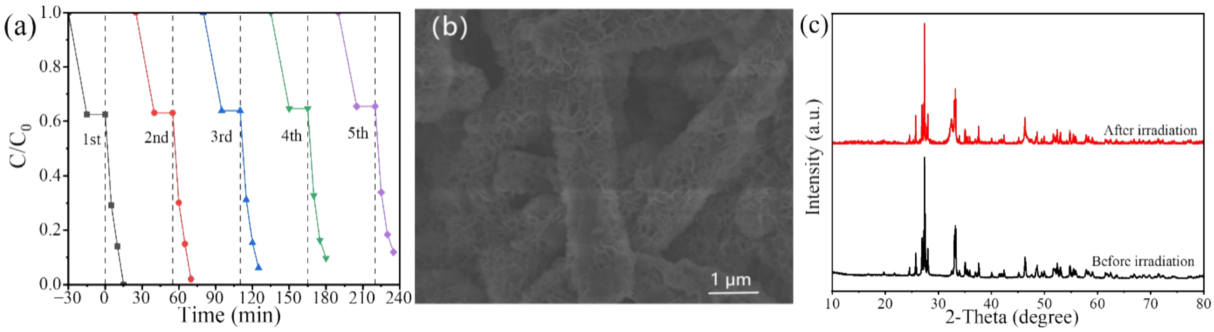

Fig. S6 (a) Cycling times for degrading Cr(VI) (50 mg•L^{-1}) with BO-2 photocatalyst, (b) SEM image and (c) XRD pattern of reducing Cr(VI) (50 mg•L^{-1}) by BO-2 sample under illumination light.

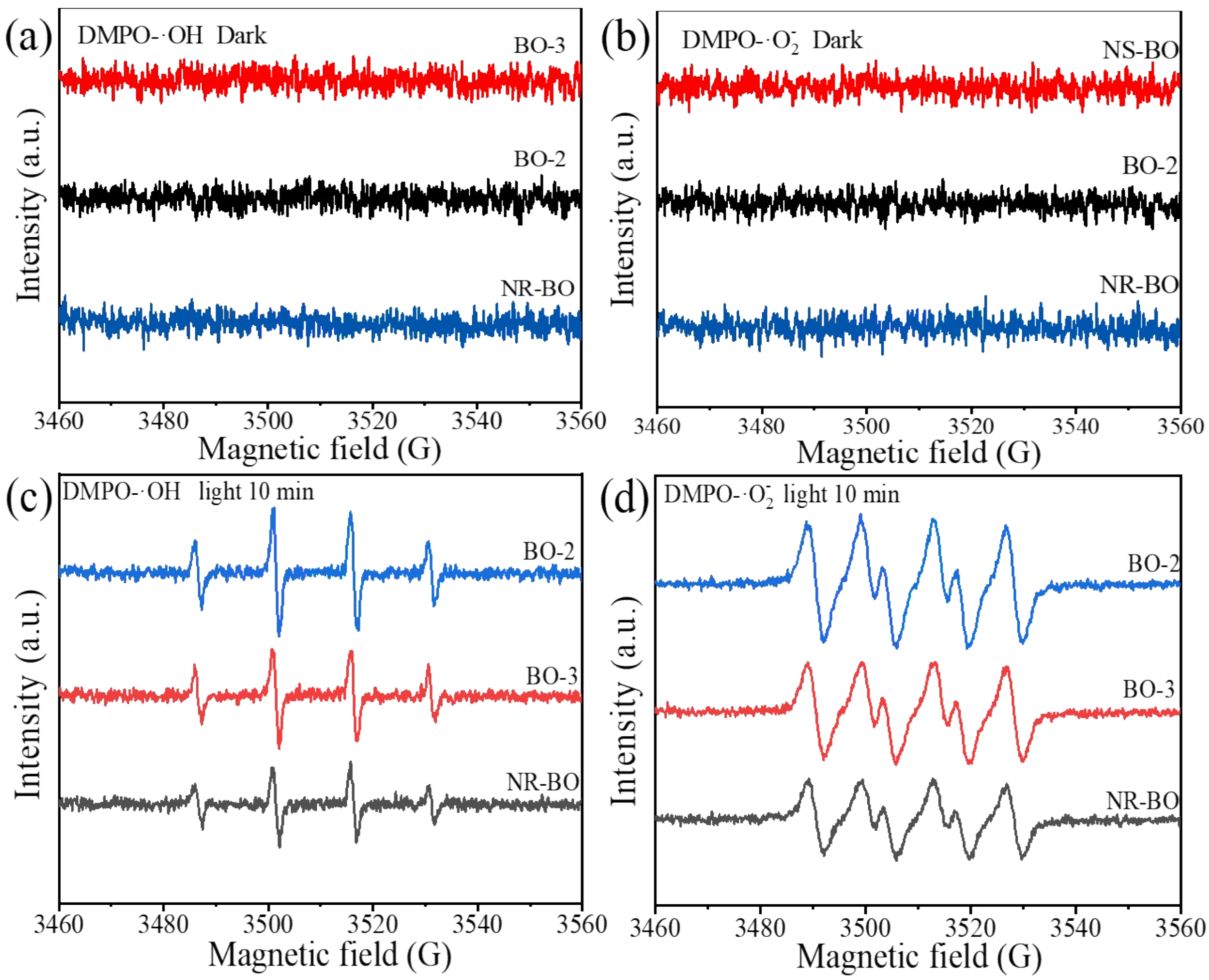

Fig. S7 In-situ ESR spectra of radical adducts trapped by (a,c) DMPO-·OH, (b,d) DMPO-·O_2^- in the obtained samples under dark and light irradiation.

Reference

1. L. Ai, D. Jia, N. Guo, M. Xu, S. Zhang, L. Wang and L. Jia, *Applied Surface Science*, 2020, **529**.
2. J. Xu, J. Yue, J. Niu and M. Chen, *Applied Surface Science*, 2019, **484**, 1080-1088.
3. R. Wang, J. Wan, J. Jia, W. Xue, X. Hu, E. Liu and J. Fan, *Materials & Design*, 2018, **151**, 74-82.
4. J. Yang, L. Chen, W. Tan, B. Han, Y. Xu, W. Wang, J. Xu and Y. Wang, *Journal of Environmental Chemical*

Engineering, 2023, **11**.
5. Y. X. Liu, C. L. Chen, Y. Q. He, Z. Zhang, M. B. Li, C. G. Li, X. B. Chen, Y. Han and Z. Shi, *Small*, 2022, **18**.
6. C. Lv, G. Chen, X. Zhou, C. Zhang, Z. Wang, B. Zhao and D. Li, *ACS Applied Materials & Interfaces*, 2017, **9**, 23748-23755.
7. Q. Meng, Y. Zhou, G. Chen, Y. Hu, C. Lv, L. Qiang and W. Xing, *Chemical Engineering Journal*, 2018, **334**, 334-343.
8. J. Xu, J. Zhu and M. Chen, *Journal of Molecular Liquids*, 2020, **320**.
9. C. Wang, H. Y. Liu, G. F. Wang, H. Y. Fang, X. G. Yuan and C. M. Lu, *Chemical Engineering Journal*, 2022, **450**.
10. D. Majhi, A. K. Mishra, K. Das, R. Bariki and B. G. Mishra, *Chemical Engineering Journal*, 2021, **413**.
11. Y. Liang, W. C. Xu, J. Z. Fang, Z. Liu, D. D. Chen, T. Pan, Y. T. Yu and Z. Q. Fang, *Applied Catalysis B-Environmental*, 2021, **295**.
12. Z. Khazaee, A. R. Mahjoub, A. H. C. Khavar, V. Srivastava and M. Sillanpää, *Environmental Science and Pollution Research*, 2021, **28**, 50747-50766.
13. Z. P. Wei, N. Zheng, X. L. Dong, X. F. Zhang, H. C. Ma, X. X. Zhang and M. Xue, *Chemosphere*, 2020, **257**.
14. K. Wang, Z. Y. Qian and W. H. Guo, *Materials Research Bulletin*, 2019, **111**, 202-211.
15. Z. Khazaee, A. R. Mahjoub, A. H. C. Khavar, V. Srivastava and M. Sillanpää, *Solar Energy*, 2020, **207**, 1282-1299.
16. Q. Wang, X. D. Shi, E. Q. Liu, J. C. Crittenden, X. J. Ma, Y. Zhang and Y. Q. Cong, *Journal of Hazardous Materials*, 2016, **317**, 8-16.
17. F. Qin, H. P. Zhao, G. F. Li, H. Yang, J. Li, R. M. Wang, Y. L. Liu, J. C. Hu, H. Z. Sun and R. Chen, *Nanoscale*, 2014, **6**, 5402-5409.
18. E. Q. Zhu, Y. H. Ma, H. Du, K. Z. Qi, M. Ainiwa and Z. Su, *Applied Surface Science*, 2020, **528**.
19. X. Q. Wang, J. Zhang, R. Wang, Y. J. Ren, S. Y. Jin, S. M. Wang, H. J. Lu, Y. J. Wang, J. Z. Zhao and C. H. Xiong, *Journal of Alloys and Compounds*, 2023, **940**.
20. J. Shang, H. G. Chen, B. Zhao, F. Zhou, H. Zhang and X. W. Wang, *Journal of Materials Science-Materials in Electronics*, 2019, **30**, 17956-17962.
21. C. F. Yu, P. Y. Yang, L. N. Tie, S. Y. Yang, S. Y. Dong, J. Y. Sun and J. H. Sun, *Applied Surface Science*, 2018, **455**, 8-17.
22. Y. Zhang, Y. C. Li, Y. Peng and J. Y. Liu, *Applied Surface Science*, 2024, **642**.